NANO EXPRESS　　　　　　　　　　　　　　　　　　　　**Open Access**

CrossMark

Suppression of Breast Cancer Cell Migration by Small Interfering RNA Delivered by Polyethylenimine-Functionalized Graphene Oxide

Yuan-Pin Huang[1], Chao-Ming Hung[2], Yi-Chiang Hsu[3,4], Cai-Yan Zhong[5], Wan-Rou Wang[5], Chi-Chang Chang[6] and Mon-Juan Lee[4,5*]

Abstract

The carbon-based nanomaterial graphene can be chemically modified to associate with various molecules such as chemicals and biomolecules and developed as novel carriers for drug and gene delivery. In this study, a nonviral gene transfection reagent was produced by functionalizing graphene oxide (GO) with a polycationic polymer, polyethylenimine (PEI), to increase the biocompatibility of GO and to transfect small interfering RNA (siRNA) against C-X-C chemokine receptor type 4 (CXCR4), a biomarker associated with cancer metastasis, into invasive breast cancer cells. PEI-functionalized GO (PEI-GO) was a homogeneous aqueous solution that remained in suspension during storage at 4 °C for at least 6 months. The particle size of PEI-GO was 172 ± 4.58 and 188 ± 5.00 nm at 4 and 25 °C, respectively, and increased slightly to 262 ± 17.6 nm at 37 °C, but remained unaltered with time. Binding affinity of PEI-GO toward siRNA was assessed by electrophoretic mobility shift assay (EMSA), in which PEI-GO and siRNA were completely associated at a PEI-GO:siRNA weight ratio of 2:1 and above. The invasive breast cancer cell line, MDA-MB-231, was transfected with PEI-GO in complex with siRNAs against CXCR4 (siCXCR4). Suppression of the mRNA and protein expression of CXCR4 by the PEI-GO/siCXCR4 complex was confirmed by real-time PCR and western blot analysis. In addition, the metastatic potential of MDA-MB-231 cells was attenuated by the PEI-GO/siCXCR4 complex as demonstrated in wound healing assay. Our results suggest that PEI-GO is effective in the delivery of siRNA and may contribute to targeted gene therapy to suppress cancer metastasis.

Keywords: Graphene oxide (GO), Polyethylenimine (PEI), Small interfering RNA (siRNA), C-X-C chemokine receptor type 4 (CXCR4), Cancer cell migration

Background

Graphene oxide (GO) is a carbon-based nanomaterial with a single layer of carbon molecules covalently linked to oxidized functional groups such as carboxyl (–COOH) and hydroxyl (–OH) groups, which can be chemically modified to increase its biocompatibility in order to associate with drugs and biomolecules [1]. Functionalized graphene oxide has been considered nanocarriers for drug delivery [2–4], combined delivery of drug and gene for cancer therapy [9–12], as well as protein transportation [13–15]. It has also been applied in biosensing [16, 17], bioimaging [18, 19], and tissue engineering [20, 21].

Polyethylenimine (PEI), a polycationic polymer that attracts nucleic acids through electrostatic interaction, is commonly used in the functionalization of nanomaterials for gene delivery. PEI-functionalized GO (PEI-GO) successfully delivered both small interfering RNA (siRNA) and anticancer drugs to enhance chemotherapeutic effect in cancer cells [9]. A noncovalent PEI-GO complex was reported to enhance GFP plasmid expression in HeLa cells [22]. By exploiting the near-infrared

* Correspondence: mjlee@mail.cjcu.edu.tw
[4]Innovative Research Center of Medicine, Chang Jung Christian University, Tainan, Taiwan
[5]Department of Bioscience Technology, Chang Jung Christian University, No. 1 Changda Rd., Gueiren District, Tainan City 71101, Taiwan
Full list of author information is available at the end of the article

Huang *et al. Nanoscale Research Letters* (2016) 11:247

Page 2 of 8

(NIR) optical absorbance of GO, photothermally controlled delivery of siRNA and plasmid DNA by GO functionalized with both PEI and polyethylene glycol (PEG) was achieved [23, 24].

Chemokine (C-X-C motif) receptor 4 (CXCR4), which is a class-A G protein-coupled receptor (GPCR), has been considered a biomarker for cancer metastasis and poor prognosis [25, 26]. Suppression of CXCR4 and its signaling axis is therefore a common strategy to inhibit cancer cell migration and metastasis [27–30]. Drug and gene delivery systems based on nanomaterials are thus designed to target against CXCR4 and facilitate cancer therapy and imaging. Anti-CXCR4 monoclonal antibody conjugated to superparamagnetic nanoparticles was applied in molecular imaging of pancreatic cancer cell lines [31]. PEG-functionalized carbon nanotube and cationic dextran-based nanoparticles were reported to deliver siRNA against CXCR4 into primary cells and animal model for colorectal cancer [32, 33]. Peptide ligands and peptide dendrimers against CXCR4 were used alone or in conjugation with nanoparticles to deliver anticancer drugs, inhibit tumor metastasis, and enhance molecular imaging [34–37]. In addition, synthetic polycationic viologen dendrimers (VGD) targeting CXCR4 were also developed to facilitate targeted delivery of plasmid DNAs and cancer therapy [38].

In this study, we explored the potential of PEI-GO in the transfection of siRNAs against CXCR4 (siCXCR4) to suppress the migration of MDA-MB-231 cells, a metastatic cancer cell line overexpressing CXCR4. Transfection efficiency was evaluated by the level of suppression of CXCR4 mRNA, as well as the migration ability of MDA-MB-231, and was compared to a commercial transfection reagent, Lipofectamine 2000. Our results suggest that PEI-GO is a potentially efficient nonviral transfection reagent that may contribute to targeted cancer therapy.

Methods

PEI Functionalization of Graphene Oxide

Graphene oxide (GO, Sigma-Aldrich, St. Louis, MO, USA) was activated with (1-ethyl-3-(3-dimethyl-amino-propyl) carbodiimide (EDC) and linked to PEI (branched, average M_W~25,000 by LS, average M_n~10,000 by GPC, Sigma-Aldrich, St. Louis, MO, USA) through the formation of amide bonds (–CONH–) using methods reported in the literature [9]. To remove unbound PEI, the reaction product was washed with ddH$_2$O and centrifuged repeatedly at 3,000 rpm for 15–30 min in an Amicon Ultra-15 Centrifugal Filter Unit (Millipore, Billerica, MA, USA) with a molecular weight cut-off of 100 kDa. The flow-through was subjected to ninhydrin assay to determine the level of free PEI.

Ninhydrin Assay

During washing of PEI-GO, 1 ml of flow-through from the Amicon Ultra-15 Centrifugal Filter Unit was mixed with 200 μl of 2 % (*w/v*) ninhydrin solution, followed by reaction in a boiling water bath for 3 min. Ninhydrin reacts with the primary and secondary amines of free PEI to produce Ruhemann's purple, which was gradually decreased with successive washing. PEI-GO was considered
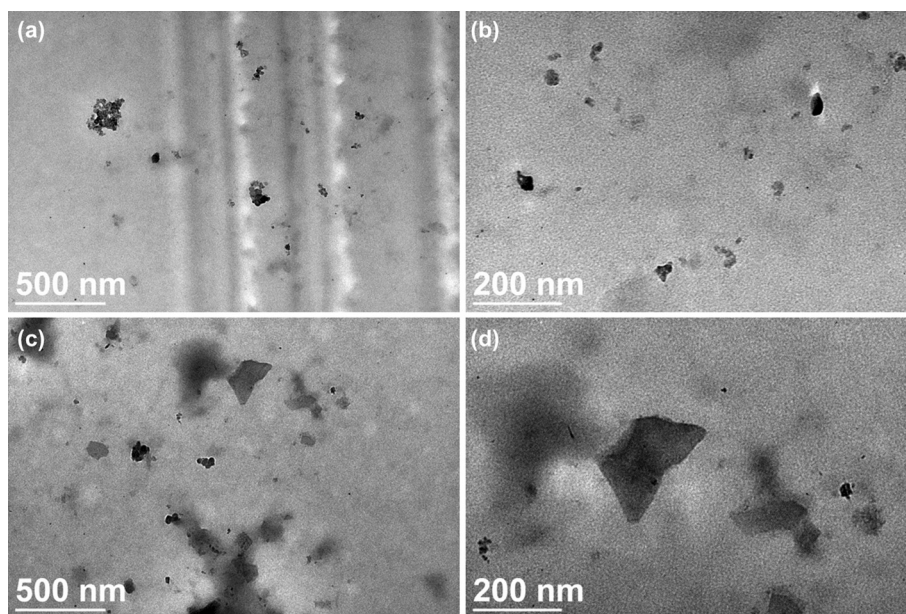
Fig. 1 Transmission electron microscopy images of pristine GO and PEI-GO. The surface morphology of pristine GO (**a**, **b**) was compared with that of PEI-GO (**c**, **d**) by a JEOL 2000FX TEM at different scales

Huang *et al. Nanoscale Research Letters* (2016) 11:247

Page 3 of 8

free of unreacted PEI when the color of Ruhemann's purple was undetectable by the naked eye.

Characterization of PEI-GO

The difference in morphology between pristine GO and PEI-GO was examined by transmission electron microscopy (JEOL 2000FX TEM) and scanning electron microscopy (JSM-6500F SEM). The particle size and zeta potential of PEI-GO were determined by dynamic light scattering using Zetasizer Nano ZS system (Malvern Instruments, Worcestershire, UK).

Electrophoretic Mobility Shift Assay (EMSA)

Dharmacon siGENOME GAPD Control siRNA (Thermo Fisher Scientific, Waltham, MA, USA) was used in EMSA to analyze the binding capacity of PEI-GO. The PEI-GO:siRNA complex was formed by incubating 0–0.6 μg of PEI-GO wi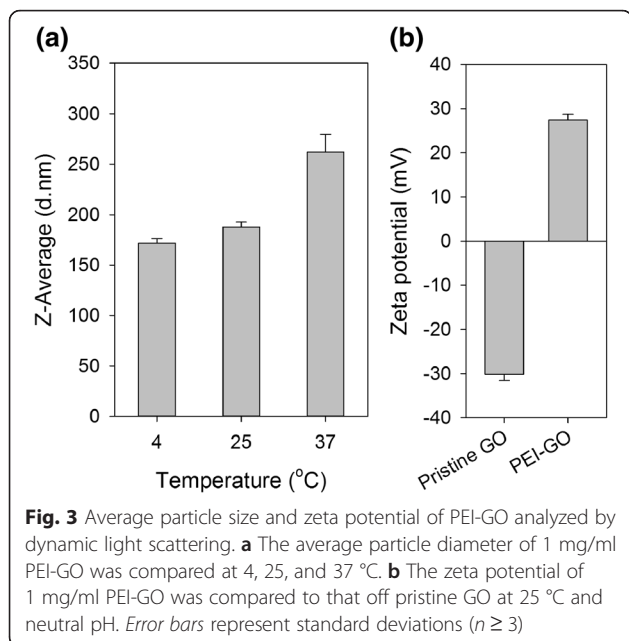th 0.2 μg siRNA at various mass ratios in serum-free cell culture medium for 20 min at room temperature. The complex was then mixed with SYBR Green I and resolved by 1 % agarose gel as described previously [39].

Cell Culture

Human breast carcinoma cell line MDA-MB-231 was cultured at 37 °C in the absence of CO_2 in Leibovitz's L-15 medium (Gibco, Life Technologies, Carlsbad, CA, USA) supplemented with 10 % fetal bovine serum (FBS), 50 units/ml penicillin, and 50 μg/ml streptomycin. The medium was refreshed every 3–4 days, and confluent cells were subcultured 7 days after seeding. Cells were seeded at 5000 cells/well in 96-well plates for cell viability assay, at 10^5 cells/well in 6-well plates for total RNA extraction, and at 2×10^4 cells/well in 24-well plates for wound healing assay.
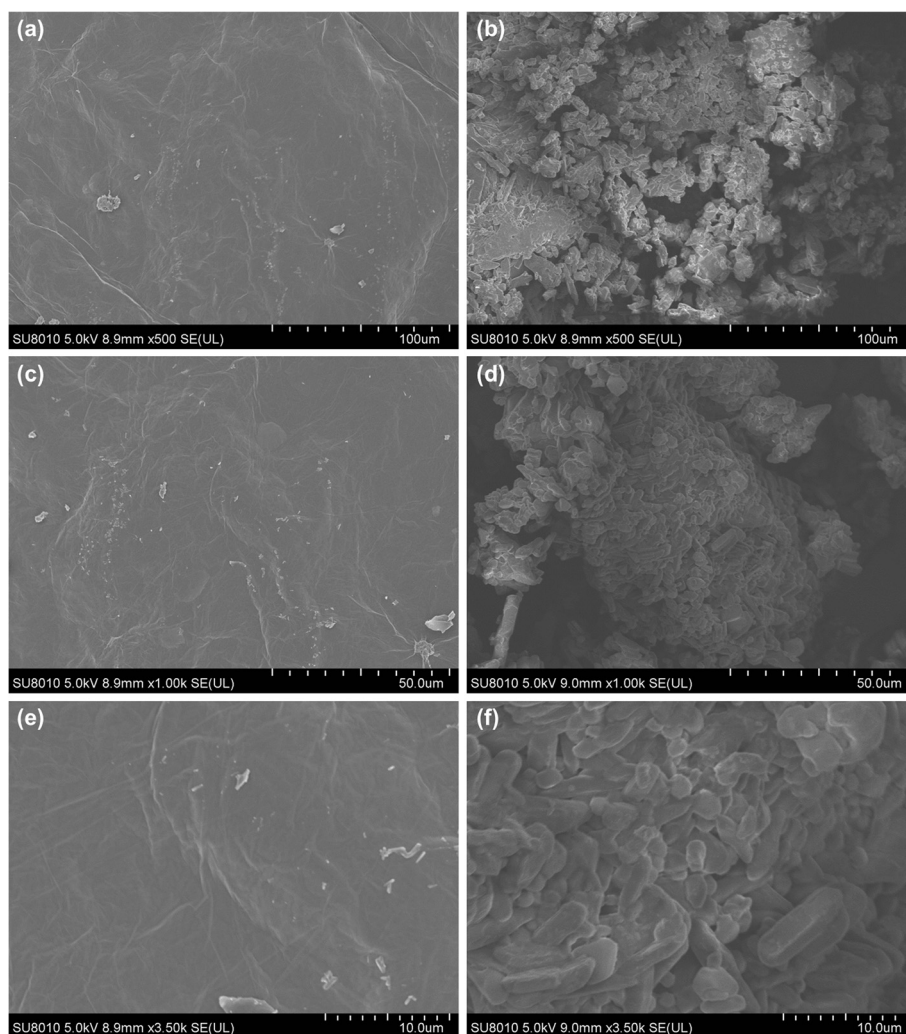
Fig. 2 Scanning electron microscopy images of pristine GO and PEI-GO. The surface morphology of pristine GO (**a**, **c**, **e**) was compared with that of PEI-GO (**b**, **d**, **f**) by a JSM-6500 F SEM at different scales

Huang *et al. Nanoscale Research Letters* (2016) 11:247

Page 4 of 8

Fig. 3 Average particle size and zeta potential of PEI-GO analyzed by dynamic light scattering. **a** The average particle diameter of 1 mg/ml PEI-GO was compared at 4, 25, and 37 °C. **b** The zeta potential of 1 mg/ml PEI-GO was compared to that off pristine GO at 25 °C and neutral pH. *Error bars* represent standard deviations ($n \geq 3$)

Cell Viability Assay

MDA-MB-231 cells were treated with 0–20 µg/ml PEI-GO for 48 h, followed by WST-1 assay using Quick Cell Proliferation Colorimetric Assay Kit (BioVision, Milpitas, CA, USA). Cell viability was quantitated spectrophotometrically by measuring the optical density at 450 nm, with a reference wavelength of 650 nm.

siRNA Transfection with PEI-GO

MDA-MB-231 cells were treated with Dharmacon siGENOME siRNA specific for human CXCR4 (siCXCR4) or siGENOME GAPD Control siRNA (siMOCK). The siRNA was delivered either by Lipofectamine 2000 (Life Technologies, Carlsbad, CA, USA) according to manufacturer's instructions or by PEI-GO. PEI-GO was incubated with siCXCR4 at mass ratios of 0.3:1, 0.5:1, and 1:1 for 20 min at room temperature before cultured with MDA-MB-231 cells to achieve a final siCXCR4 concentration of

25 nM. Two days after siRNA transfection, cells were harvested for RNA extraction and real-time PCR analysis or subjected to wound healing assay.
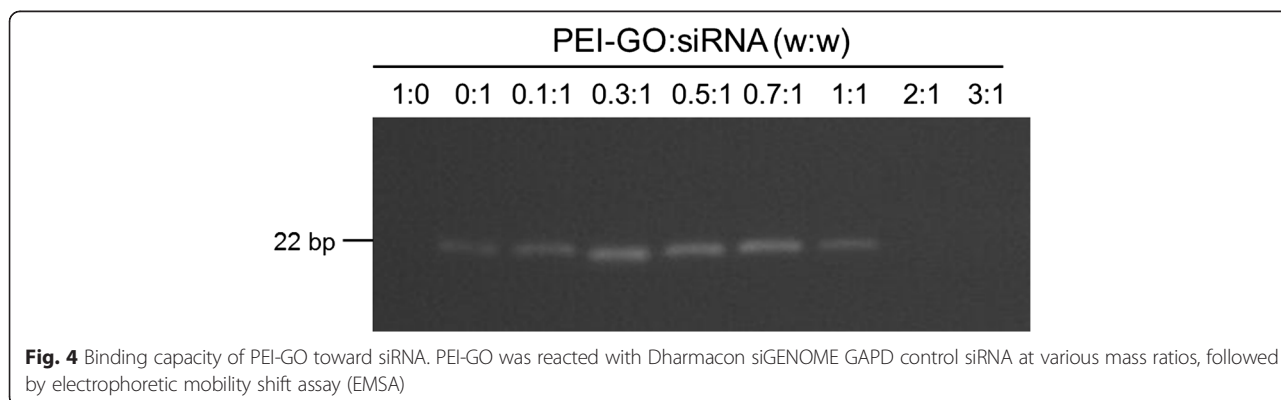
Real-Time Polymerase Chain Reaction

Total RNA was isolated by PureLink® RNA Mini Kit (Thermo Fisher Scientific, Waltham, MA, USA), and cDNA synthesis was carried out using the SuperScript III First-Strand Synthesis SuperMix for qRT-PCR (Life Technologies, Carlsbad, CA, USA) according to the manufacturer's instructions. The cDNA was diluted to a final concentration of ~1 ng/µl and reacted with CXCR4 (NM_003467)- or GAPDH (NM_002046.4)-specific primer pairs and Quanti-Fast SYBR® Green PCR Kit (QIAGEN, Germantown, MD, USA). PCR was performed by Applied Biosystems 7300 Real-Time PCR System and monitored with Applied Biosystems Sequence Detection Software V1.2 (Life Technologies, Carlsbad, CA, USA) as described previously [40].
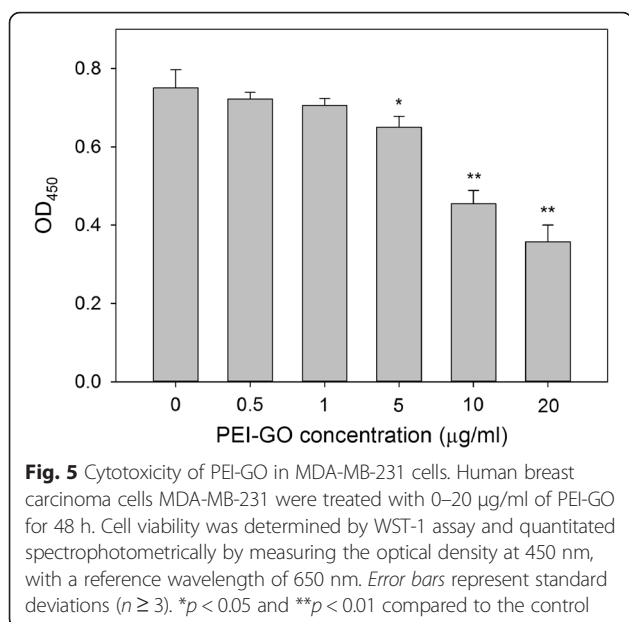
Wound Healing Assay

Wound healing assay was performed by following the protocol provided in the literature [41]. MDA-MB-231 cells were cultured in a 24-well plate and treated with siCXCR4 or siMOCK complexed with either PEI-GO or Lipofectamine 2000 for 48 h. The cell monolayer in each well was scraped with a p200 pipet tip to create a gap. After washing with culture medium to remove cell debris, the cells were allowed to migrate for 24 h, followed by observation under an Olympus CKX41 optical microscope.

Statistical Analysis

Statistical analysis was performed on data from at least three independent experiments. Significant difference relative to the control was tested using Student's *t* test. Levels of significance of $p < 0.05$ and 0.01 were accepted as significant and highly significant, respectively.

Fig. 4 Binding capacity of PEI-GO toward siRNA. PEI-GO was reacted with Dharmacon siGENOME GAPD control siRNA at various mass ratios, followed by electrophoretic mobility shift assay (EMSA)

Huang *et al. Nanoscale Research Letters* (2016) 11:247

Page 5 of 8

Fig. 5 Cytotoxicity of PEI-GO in MDA-MB-231 cells. Human breast carcinoma cells MDA-MB-231 were treated with 0–20 μg/ml of PEI-GO for 48 h. Cell viability was determined by WST-1 assay and quantitated spectrophotometrically by measuring the optical density at 450 nm, with a reference wavelength of 650 nm. *Error bars* represent standard deviations ($n \geq 3$). *$p < 0.05$ and **$p < 0.01$ compared to the control

Results

Characterization of PEI-GO

PEI functionalization increased the hydrophilicity and dispersibility of GO, which formed aggregates and precipitated in water prior to functionalization. The PEI-GO suspension can be maintained for at least 10 months without precipitation. As examined by transmission electron microscopy and scanning electron microscopy, pristine GO was tightly packed (Fig. 1a, b) and had a relatively smooth surface (Fig. 2a, c, e). PEI functionalization increased the surface area of PEI-GO, as well as the spacing between graphene layers, which appeared more extended (Fig. 1c, d) and was highly agglomerated, indicating that the stacking of the graphene sheets was disturbed (Fig. 2b, d, f). The particle size of PEI-GO was 172 ± 4.58 and 188 ± 5.00 nm at 4 and 25 °C, respectively, and increased slightly to 262 ± 17.6 nm at 37 °C (Fig. 3a), suggesting that that PEI-GO may be partially aggregated in cell culture. However, when the particle size immediately after synthesis was compared to that after stored at 4 °C for over 10 months, no significant change was observed (data not shown). As shown in Fig. 3b, the zeta potential of pristine GO was negative (-30.2 ± 1.34 mV), while that of PEI-GO was positive (27.4 ± 1.25 mV), indicating that PEI functionalization increased the positive charge on the surface of GO and contributed to the electrostatic repulsion that stabilized the PEI-GO suspension.

Binding Capacity of PEI-GO to siRNA

Binding capacity of PEI-GO toward siRNA was assessed by electrophoretic mobility shift assay (EMSA). PEI-GO was complexed with siRNA at various mass ratios and resolved

with agarose gel electrophoresis (Fig. 4). Binding of siRNA to PEI-GO resulted in reduced mobility of free siRNAs and their availability for SYBR Green I intercalation. As the amount of PEI-GO increased, more siRNAs were adsorbed, resulting in decreased fluorescence signal of free siRNAs. The migration of siRNA was completely inhibited when the mass ratio of PEI-GO:siRNA was 2:1 and above.

Cytotoxicity of PEI-GO

The cytotoxicity of PEI-GO in MDA-MB-231 cells, a invasive breast cancer cell line, was analyzed by WST-1 assay. After incubated with PEI-GO for 48 h, we observed that the viability of MDA-MB-231 cells decreased with increasing concentrations of PEI-GO (Fig. 5). In the presence of 20 μg/ml PEI-GO, the number of viable cells reduced to 47.6 % of that of the control. The final concentration of PEI-GO in siRNA transfection was therefore limited within the range which had no significant effect on cell viability.

Suppression of CXCR4 by siCXCR4 Transfected with PEI-GO

The transfection efficiency of PEI-GO compared to Lipofectamine 2000 was demonstrated by delivering siCXCR4 into MDA-MB-231 cells. After siCXCR4 treatment for
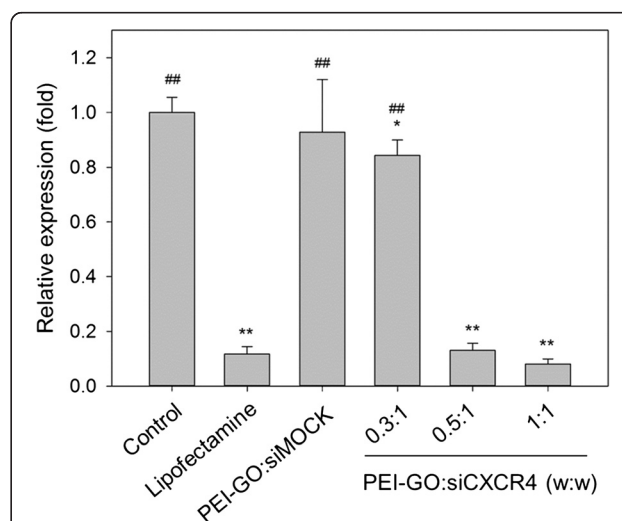
Fig. 6 Relative CXCR4 mRNA expression of MDA-MB-231 cells transfected with PEI-GO:siCXCR4 complexes. PEI-GO was incubated with siCXCR4 at mass ratios of 0.3:1, 0.5:1, and 1:1 for 20 min at room temperature before cultured with MDA-MB-231 cells to achieve a final siCXCR4 concentration of 25 nM. Two days after siRNA transfection, cells were harvested for RNA extraction and real-time PCR analysis. Control, MDA-MB-231 cells cultured in growth medium for 48 h; Lipofectamine, MDA-MB-231 cells transfected with siCXCR4 using Lipofectamine 2000 as transfection reagent; PEI-GO:siMOCK, MDA-MB-231 cells transfected with PEI-GO:siMOCK at a mass ratio of 1:1. *Error bars* represent standard deviations ($n \geq 3$). *$p < 0.05$ and **$p < 0.01$ compared to the control; ##$p < 0.01$ compared to Lipofectamine

Huang *et al. Nanoscale Research Letters* (2016) 11:247

Page 6 of 8

48 h, CXCR4 mRNA expression reduced significantly to 13 and 8 % of untreated control at PEI-GO:siCXCR4 mass ratios of 0.5:1 and 1:1, respectively, but was nearly unaffected at a PEI-GO:siCXCR4 ratio of 0.3:1, and in the presence of siMOCK, a nonspecific siRNA control (Fig. 6). Transfection efficiency of PEI-GO was comparable to that of the Lipofectamine:siCXCR4 complex, which reduced CXCR4 expression to 12 % of control. These results suggest that at appropriate mass ratios, target-specific and efficient transfection can be achieved by PEI-GO.

Effect of siCXCR4 Transfected by PEI-GO on Cell Migration

The effect of CXCR4 suppression on cell migration was examined by wound healing assay. MDA-MB-231 cells transfected with siCXCR4 were allowed to migrate in a cell-free gap created in the culture plate. For untreated cells or those treated with siMOCK, the gap was filled with migrated cells after 24 h (Fig. 7a, c). When the mRNA expression of CXCR4 was suppressed by siCXCR4, fewer cells were present in the gap, indicating that cell migration was retarded. As shown in Fig. 7d–f, siCXCR4 delivered by PEI-GO suppressed the migration of MDA-MB-231 cells at PEI-GO:siCXCR4 ratios of 0.5:1 and 1:1, but the effect was insignificant when the PEI-GO:siCXCR4 ratio was 0.3:1, consistent with the results of CXCR4 gene expression (Fig. 6). In addition, the extent of migrational suppression resulted from PEI-GO:siCXCR4 was comparable to that of the Lipofectamine:siCXCR4 complexes (Fig. 7g).
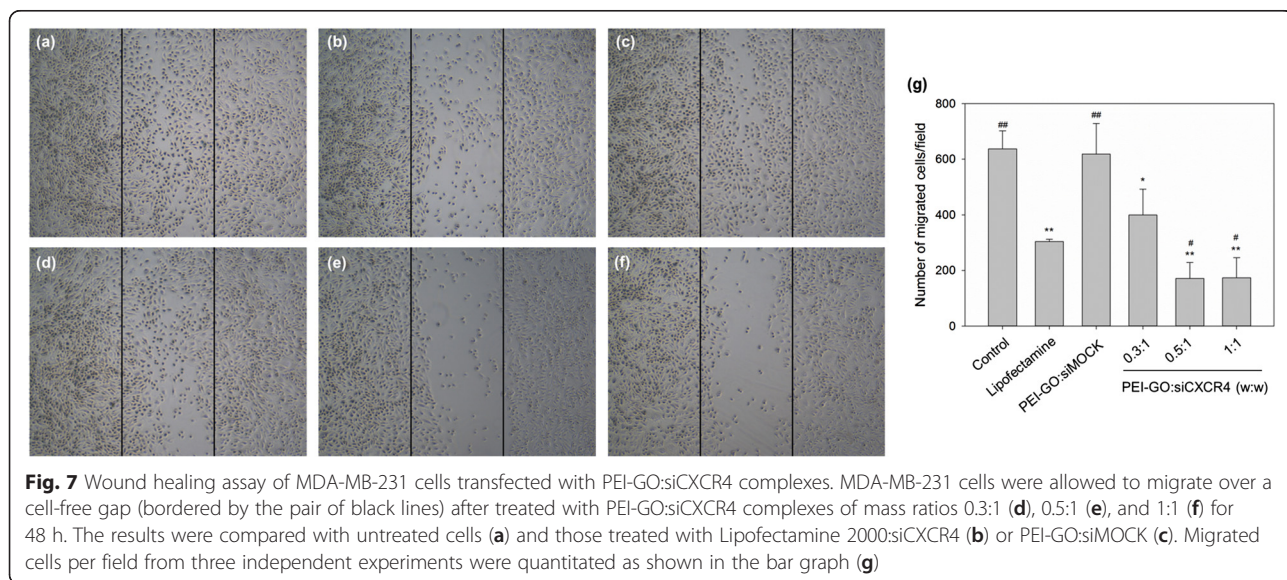
Discussion

With improved vector designs, recent clinical trials have eliminated the safety concerns of gene therapy and demonstrated remarkable therapeutic benefits in inherited diseases of the blood and immune and nervous systems [42]. Gene therapy is expected to become a new approach to the development of novel therapeutic strategies beyond conventional methods. Although current strategies on clinical gene therapy are based predominantly on viral vectors, nonviral transfection reagents provide safer alternatives without potential side effects such as immunogenicity and carcinogenesis that are associated with viral transfection [43].

In this study, we demonstrated that PEI-GO is an effective nonviral carrier for siRNA delivery and may potentially be applied in targeted gene therapy to suppress cancer metastasis. Interestingly, studies have shown that pristine graphene or GO, as well as polyethylene glycol (PEG)-modified GO (PEG-GO) inhibit breast cancer cell migration through impairment of oxidative phosphorylation and mitochondrial respiration [44, 45]. In addition, GO selectively targets and retards the clonal expansion of multiple cancer stem cells [46]. These results indicate that GO alone is capable of suppressing cancer metastasis and tumor development. However, because a relatively lower concentration of PEI-GO was used in this study (0.3 µg/ml PEI-GO compared to 40 or 80 µg/ml PEG-GO in the literature), inhibition of cell migration was not observed when MDA-MB-231 cells were treated with PEI-GO alone.

Conclusions

Our results indicate that PEI-GO is capable of delivering siCXCR4 to suppress gene expression and metastatic potential of MDA-MB-231 cells. PEI-GO may be developed as a novel nonviral transfection reagent that contributes to targeted gene therapy to suppress cancer metastasis.

Fig. 7 Wound healing assay of MDA-MB-231 cells transfected with PEI-GO:siCXCR4 complexes. MDA-MB-231 cells were allowed to migrate over a cell-free gap (bordered by the pair of black lines) after treated with PEI-GO:siCXCR4 complexes of mass ratios 0.3:1 (**d**), 0.5:1 (**e**), and 1:1 (**f**) for 48 h. The results were compared with untreated cells (**a**) and those treated with Lipofectamine 2000:siCXCR4 (**b**) or PEI-GO:siMOCK (**c**). Migrated cells per field from three independent experiments were quantitated as shown in the bar graph (**g**)

Huang *et al. Nanoscale Research Letters* (2016) 11:247

Page 7 of 8

Author details
[1]Department of Cosmetics and Fashion Styling, Cheng Shiu University, Kaohsiung, Taiwan. [2]Department of General Surgery, E-Da Hospital, Kaohsiung, Taiwan. [3]Graduate Institute of Medical Sciences, Chang Jung Christian University, Tainan, Taiwan. [4]Innovative Research Center of Medicine, Chang Jung Christian University, Tainan, Taiwan. [5]Department of Bioscience Technology, Chang Jung Christian University, No. 1 Changda Rd., Gueiren District, Tainan City 71101, Taiwan. [6]Department of Obstetrics and Gynecology, E-Da Hospital, Kaohsiung, Taiwan.

References
1. Zhou X, Liang F (2014) Application of graphene/graphene oxide in biomedicine and biotechnology. Curr Med Chem 21:855–69
2. Liu J, Cui L, Losic D (2013) Graphene and graphene oxide as new nanocarriers for drug delivery applications. Acta Biomater 9:9243–57
3. Zhang L, Xia J, Zhao Q, Liu L, Zhang Z (2010) Functional graphene oxide as a nanocarrier for controlled loading and targeted delivery of mixed anticancer drugs. Small 6:537–44
4. Liu Z, Robinson JT, Sun X, Dai H (2008) PEGylated nanographene oxide for delivery of water-insoluble cancer drugs. J Am Chem Soc 130:10876–7
5. Yin D, Li Y, Lin H, Guo B, Du Y, Li X et al (2013) Functional graphene oxide as a plasmid-based Stat3 siRNA carrier inhibits mouse malignant melanoma growth in vivo. Nanotechnology 24:105102
6. Imani R, Emami SH, Faghihi S (2015) Synthesis and characterization of an octaarginine functionalized graphene oxide nano-carrier for gene delivery applications. Phys Chem Chem Phys 17:6328–39
7. Paul A, Hasan A, Kindi HA, Gaharwar AK, Rao VT, Nikkhah M et al (2014) Injectable graphene oxide/hydrogel-based angiogenic gene delivery system for vasculogenesis and cardiac repair. ACS Nano 8:8050–62
8. Yang X, Niu G, Cao X, Wen Y, Xiang R, Duana H et al (2012) The preparation of functionalized graphene oxide for targeted intracellular delivery of siRNA. J Mater Chem 22:6649–54
9. Zhang L, Lu Z, Zhao Q, Huang J, Shen H, Zhang Z (2011) Enhanced chemotherapy efficacy by sequential delivery of siRNA and anticancer drugs using PEI-grafted graphene oxide. Small 7:460–4
10. Bao H, Pan Y, Ping Y, Sahoo NG, Wu T, Li L et al (2011) Chitosan-functionalized graphene oxide as a nanocarrier for drug and gene delivery. Small 7:1569–78
11. Zhi F, Dong H, Jia X, Guo W, Lu H, Yang Y et al (2013) Functionalized graphene oxide mediated adriamycin delivery and miR-21 gene silencing to overcome tumor multidrug resistance in vitro. PLoS One 8:e60034
12. Cao X, Zheng S, Zhang S, Wang Y, Yang X, Duan H et al (2015) Functionalized Graphene Oxide with Hepatocyte Targeting as Anti-Tumor Drug and Gene Intracellular Transporters. J Nanosci Nanotechnol 15:2052–9
13. Kim S, Ryoo SR, Na HK, Kim YK, Choi BS, Lee Y et al (2013) Deoxyribozyme-loaded nano-graphene oxide for simultaneous sensing and silencing of the hepatitis C virus gene in liver cells. Chem Commun (Camb) 49:8241–3
14. Jana B, Mondal G, Biswas A, Chakraborty I, Saha A, Kurkute P et al (2013) Dual functionalized graphene oxide serves as a carrier for delivering oligohistidine- and biotin-tagged biomolecules into cells. Macromol Biosci 13:1478–84
15. Shen H, Liu M, He H, Zhang L, Huang J, Chong Y et al (2012) PEGylated graphene oxide-mediated protein delivery for cell function regulation. ACS Appl Mater Interfaces 4:6317–23
16. Wang Y, Li Z, Hu D, Lin CT, Li J, Lin Y (2010) Aptamer/graphene oxide nanocomplex for in situ molecular probing in living cells. J Am Chem Soc 132:9274–6
17. Zhang J, Sun Y, Xu B, Zhang H, Gao Y, Zhang H et al (2013) A novel surface plasmon resonance biosensor based on graphene oxide decorated with gold nanorod-antibody conjugates for determination of transferrin. Biosens Bioelectron 45:230–6
18. Kim H, Namgung R, Singha K, Oh IK, Kim WJ (2011) Graphene oxide-polyethylenimine nanoconstruct as a gene delivery vector and bioimaging tool. Bioconjug Chem 22:2558–67
19. Sun X, Liu Z, Welsher K, Robinson JT, Goodwin A, Zaric S et al (2008) Nano-Graphene Oxide for Cellular Imaging and Drug Delivery. Nano Res 1:203–12
20. Ku SH, Park CB (2013) Myoblast differentiation on graphene oxide. Biomaterials 34:2017–23
21. Lee WC, Lim CH, Shi H, Tang LA, Wang Y, Lim CT et al (2011) Origin of enhanced stem cell growth and differentiation on graphene and graphene oxide. ACS Nano 5:7334–41
22. Feng L, Zhang S, Liu Z (2011) Graphene based gene transfection. Nanoscale 3:1252–7
23. Kim H, Kim WJ (2014) Photothermally controlled gene delivery by reduced graphene oxide-polyethylenimine nanocomposite. Small 10:117–26
24. Feng L, Yang X, Shi X, Tan X, Peng R, Wang J et al (2013) Polyethylene glycol and polyethylenimine dual-functionalized nano-graphene oxide for photothermally enhanced gene delivery. Small 9:1989–97
25. Mukherjee D, Zhao J (2013) The Role of chemokine receptor CXCR4 in breast cancer metastasis. Am J Cancer Res 3:46–57
26. Yang P, Liang SX, Huang WH, Zhang HW, Li XL, Xie LH et al (2014) Aberrant expression of CXCR4 significantly contributes to metastasis and predicts poor clinical outcome in breast cancer. Curr Mol Med 14:174–84
27. Yu ZH, Liu T, Zhao YH, Huang YY, Gao YT (2014) Cisplatin targets the stromal cell-derived factor-1-CXC chemokine receptor type 4 axis to suppress metastasis and invasion of ovarian cancer-initiating cells. Tumour Biol 35:4637–44
28. Han AR, Lee JY, Kim HJ, Min WS, Park G, Kim SH (2015) A CXCR4 antagonist leads to tumor suppression by activation of immune cells in a leukemia-induced microenvironment. Oncol Rep 34(6):2880–8
29. Zhan Y, Zhang H, Li J, Zhang Y, Zhang J, He L (2015) A novel biphenyl urea derivate inhibits the invasion of breast cancer through the modulation of CXCR4. J Cell Mol Med 19:1614–23
30. Niu J, Huang Y, Zhang L (2015) CXCR4 silencing inhibits invasion and migration of human laryngeal cancer Hep-2 cells. Int J Clin Exp Pathol 8:6255–61
31. He Y, Song W, Lei J, Li Z, Cao J, Huang S et al (2012) Anti-CXCR4 monoclonal antibody conjugated to ultrasmall superparamagnetic iron oxide nanoparticles in an application of MR molecular imaging of pancreatic cancer cell lines. Acta Radiol 53:1049–58
32. Abedini F, Hosseinkhani H, Ismail M, Domb AJ, Omar AR, Chong PP et al (2012) Cationized dextran nanoparticle-encapsulated CXCR4-siRNA enhanced correlation between CXCR4 expression and serum alkaline phosphatase in a mouse model of colorectal cancer. Int J Nanomedicine 7:4159–68
33. Liu Z, Winters M, Holodniy M, Dai H (2007) siRNA delivery into human T cells and primary cells with carbon-nanotube transporters. Angew Chem Int Ed Engl 46:2023–7
34. Chittasupho C, Lirdprapamongkol K, Kewsuwan P, Sarisuta N (2014) Targeted delivery of doxorubicin to A549 lung cancer cells by CXCR4 antagonist conjugated PLGA nanoparticles. Eur J Pharm Biopharm 88:529–38
35. Tarasov SG, Gaponenko V, Howard OM, Chen Y, Oppenheim JJ, Dyba MA et al (2011) Structural plasticity of a transmembrane peptide allows self-assembly into biologically active nanoparticles. Proc Natl Acad Sci U S A 108:9798–803
36. Kuil J, Buckle T, Oldenburg J, Yuan H, Borowsky AD, Josephson L et al (2011) Hybrid peptide dendrimers for imaging of chemokine receptor 4 (CXCR4) expression. Mol Pharm 8:2444–53
37. Gallo J, Kamaly N, Lavdas I, Stevens E, Nguyen QD, Wylezinska-Arridge M et al (2014) CXCR4-targeted and MMP-responsive iron oxide nanoparticles for enhanced magnetic resonance imaging. Angew Chem Int Ed Engl 53:9550–4
38. Li J, Lepadatu AM, Zhu Y, Ciobanu M, Wang Y, Asaftei SC et al (2014) Examination of structure-activity relationship of viologen-based dendrimers as CXCR4 antagonists and gene carriers. Bioconjug Chem 25:907–17

Huang *et al. Nanoscale Research Letters* (2016) 11:247

Page 8 of 8

39. Huang YP, Lin IJ, Chen CC, Hsu YC, Chang CC, Lee MJ (2013) Delivery of small interfering RNAs in human cervical cancer cells by polyethylenimine-functionalized carbon nanotubes. Nanoscale Res Lett 8:267
40. Tsai YH, Lin KL, Huang YP, Hsu YC, Chen CH, Chen Y et al (2015) Suppression of ornithine decarboxylase promotes osteogenic differentiation of human bone marrow-derived mesenchymal stem cells. FEBS Lett 589:2058–65
41. Liang CC, Park AY, Guan JL (2007) In vitro scratch assay: a convenient and inexpensive method for analysis of cell migration in vitro. Nat Protoc 2:329–33
42. Naldini L (2015) Gene therapy returns to centre stage. Nature 526:351–60
43. Yin H, Kanasty RL, Eltoukhy AA, Vegas AJ, Dorkin JR, Anderson DG (2014) Non-viral vectors for gene-based therapy. Nat Rev Genet 15:541–55
44. Zhou T, Zhang B, Wei P, Du Y, Zhou H, Yu M et al (2014) Energy metabolism analysis reveals the mechanism of inhibition of breast cancer cell metastasis by PEG-modified graphene oxide nanosheets. Biomaterials 35:9833–43
45. Zhou H, Zhang B, Zheng J, Yu M, Zhou T, Zhao K et al (2014) The inhibition of migration and invasion of cancer cells by graphene via the impairment of mitochondrial respiration. Biomaterials 35:1597–607
46. Fiorillo M, Verre AF, Iliut M, Peiris-Pages M, Ozsvari B, Gandara R et al (2015) Graphene oxide selectively targets cancer stem cells, across multiple tumor types: implications for non-toxic cancer treatment, via "differentiation-based nano-therapy". Oncotarget 6:3553–62